Bicosomes: Bicelles in Dilute Systems

Gelen Rodríguez,[†] Guadalupe Soria,[‡] Elisenda Coll,[§] Laia Rubio,[†] Lucyanna Barbosa-Barros,[†] Carmen López-Iglesias,[§] Anna M. Planas,[‡] Joan Estelrich,[¶] Alfons de la Maza,[†] and Olga López[†*]

[†]Departament de Tecnologia Química i de Tensioactius, Institut de Química Avançada de Catalunya, Consejo Superior de Investigaciones Científicas, Barcelona, Spain; [‡]Departament d'Isquèmia Cerebral i Neurodegeneració, Institut d'Investigacions Biomèdiques de Barcelona, Institut d'Investigatigacions Biomèdiques Agust Pi i Sunyer, Barcelona, Spain; and [§]Serveis Cientificotècnics and [¶]Departamento de Fisicoquímica, Facultad de Farmacia, Universidad de Barcelona, Barcelona, Spain

ABSTRACT Bicelles are discoidal phospholipid nanostructures at high lipid concentrations. Under dilute conditions, bicelles become larger and adopt a variety of morphologies. This work proposes a strategy to preserve the discoidal morphology of bicelles in environments with high water content. Bicelles were formed in concentrated conditions and subsequently encapsulated in liposomes. Later dilution of these new structures, called bicosomes, demonstrated that lipid vesicles were able to isolate and protect bicelles entrapped inside them from the medium. Characterization of systems before and after dilution by dynamic light-scattering spectroscopy and cryo-transmission electron microscopy showed that free bicelles changed in size and morphology, whereas encapsulated bicelles remained unaltered by the effect of dilution. Free and entrapped bicelles (containing the paramagnetic contrast agent gadodiamide) were injected into rat brain lateral ventricles. Coronal and sagittal visualization was performed by magnetic resonance imaging. Whereas rats injected with free bicelles did not survive the surgery, those injected with bicosomes did, and a hyperintensity effect due to gadodiamide was observed in the cerebrospinal fluid. These results indicate that bicosomes are a good means of preserving the morphology of bicelles under dilution conditions.

INTRODUCTION

Bicellar systems are composed of new discoidal nanostructures that consist of a phospholipid with a long hydrocarbon chain situated in a bilaminar, flat center with a short-chained phospholipid located at the edges (1). The characteristics of these bicellar systems, such as their solely lipid content, organization into a bilayer, and property of aligning in a magnetic field, have permitted the wide use of these systems as membrane models in diverse conformational studies of proteins and membrane peptides (2). In recent works (3–5), we proposed the use of phospholipid bicelles for dermatological applications because their small size allows them to pass through the skin. These studies demonstrated that bicelles affect the skin barrier differently depending on different compositional variables, working as permeabilizing agents of the skin or as reinforcing agents of the lipid structures of this tissue. In addition to using bicelles as skin barrier-function modulators, the possibility of incorporating drugs and other bioactive compounds into bicelles is being explored. In one study, drugs were incorporated into bicelles to study drug-membrane interactions (6). Another recent work focused on the percutaneous absorption of diclofenac encapsulated in bicelles (7). The incorporation of this drug results in systems that have smaller diameters and can maintain structural and chemical stability at least for 1 week. Therefore, bicelles can be considered good carriers for skin applications. Their application as carriers for administration through the systemic route, where the water content is high, arises as the next challenge. Depending on the total lipid concentration, the temperature, and the molar ratio between long- and short-chain phospholipids, bicelles can exhibit different morphologies. Under high-dilution conditions, small discoidal bicelles become large structures, such as vesicles, lamellar sheets, and rodlike micelles (4). This behavior could hinder the application of these systems by specific systemic routes because the properties of bicellar systems would be lost under diluted conditions, and the possible damage that the aforementioned structures could cause is not clear. To maintain the size and shape of the small discoidal bicelles, we propose that they be encapsulated in lipid vesicles.

Liposomes have been the subject of numerous studies because of their importance as models for more-complex biological membranes, their potential use as microencapsulators for drug delivery, and their applications in cosmetics and clinical use (8–11). These structures, with diameters ranging from 100 nm to 1 μm, are too large to pass through the skin for transdermal application. However, they are morphologically stable under high-dilution conditions and thus are good carriers for systemic application.

In this work we propose a new nanostructure: bicelles encapsulated in liposomes. These structures, termed bicosomes, unite the advantages of disks and vesicles, providing a good system for application in diluted environments. Characterization of the systems was carried out by means of dynamic light scattering (DLS) and cryo-transmission electron microscopy (cryo-TEM). The first technique was used to determine the average size of the systems, whereas the second was valuable for characterizing the dimensional and morphological aspects of the nanostructures, and

Submitted December 22, 2009, and accepted for publication March 31, 2010.

*Correspondence: oloesl@cid.csic.es

Editor: Mark Girvin.

0006-3495/10/07/0480/9 $2.00

doi: 10.1016/j.bpj.2010.03.072

obtaining a direct visualization of the lipid samples. Additionally, in vitro and in vivo experiments were conducted to determine the stability of these new structures. For in vivo experiments, a paramagnetic contrast agent (gadodiamide) was included in these systems. This agent has been used in previous studies with similar purposes (12). In this work, gadodiamide was stereotactically injected into the ventricular system of rat brains and visualized by magnetic resonance imaging (MRI). The gadodiamide-induced hyperintensity, observed by MRI, was quantified by defining a region of interest (ROI) in the cerebrospinal fluid (CSF) compartment. The goal of this study was to improve the stability of bicelles in dilute environments so that these nanostructures can be applied through different systemic routes.

MATERIALS AND METHODS

Chemicals

1,2-Dipalmitoyl-*sn*-glycero-3-phosphocholine (DPPC) and 1,2-dihexanoyl-*sn*-glycero-3-phosphocholine (DHPC) were purchased from Avanti Polar Lipids (Alabaster, AL). Lipoid S-100, whose main component (>94%) is soybean phosphatidylcholine (PC), was obtained from Lipoid GmbH (Ludwigshafen, Germany), and cholesterol (CHO) was obtained from Sigma-Aldrich-Fluka (Munich, Germany). Purified water was obtained by means of an ultrapure water system (Milli-Q plus 185; Millipore, Bedford, MA). Chloroform was purchased from Merck. Gadolinium-diethylenetriaminepentaacetic acid (gadodiamide, Omniscan) was supplied by GE-Healthcare (Barcelona, Spain).

Preparation of systems

Bicelles

Samples were prepared by mixing appropriate amounts of DPPC powder and a DHPC chloroform solution to reach a DPPC/DHPC molar ratio $q = 3.5$. After the components were mixed, the chloroform was removed with a rotary evaporator and the systems were hydrated with an aqueous solution of the paramagnetic marker gadodiamide to reach a 20% (w/v) total lipid concentration. Bicellar solutions were prepared by subjecting the samples to several cycles of sonication and freezing until the samples became transparent (4).

Bicelles encapsulated in liposomes (bicosomes)

The liposome composition consisted of 80% Lipoid S-100 and 20% cholesterol. These two components were mixed in chloroform, and afterward a lipid film was formed by removing the chloroform by rotary evaporation. The film was hydrated with the previously formed bicellar solution. These solutions were extruded three times through 800-nm polycarbonate membranes. The liposome solution was centrifuged for 45 min at 20,000 $\times$ *g* in a Labnet spectrafuge 16M. This separated the gadodiamide-including lipid systems from non-gadodiamide-including ones, and also formed the majority of the nonencapsulated bicelles.

Control liposomes were formed according to the same methods, with the exception that the film was hydrated with an aqueous solution of the paramagnetic marker gadodiamide.

Characterization of the systems

To evaluate the effect of dilution in the systems, samples were analyzed by DLS and Cryo-TEM before and after dilution.

DLS

The hydrodynamic diameter (HD) and polydispersity index (PI) were determined by means of DLS using a Zetasizer Nano ZS90 (Malvern Systems, Southborough, MA). The DLS technique measures the Brownian motion of the particles and correlates it to the particle sizes. The relationship between a particle size and its diffusion coefficient due to Brownian motion is defined in the Stokes-Einstein equation:

$$HD = kT/3\,\pi\eta\,D$$

where D is the translational diffusion coefficient (m^2/s), k is Boltzmann's constant ($1.3806503 \times 10^{-23}\ m^2\ kg\ s^{-2}\ k^{-1}$), T is the absolute temperature (K), and η is the viscosity (mPa.s). The different sizes were determined by detection and analysis of scattered light when the 632-nm He/Ne laser beam crossed the sample.

The interpretation of data was performed considering the size distribution by intensity and by volume of the scattered light. The use of this technique, which considers that particles with different sizes scatter different intensities of light, is especially useful in samples with extensive size heterogeneity. The measurements by DLS were performed at 25°C and 37°C to observe the characteristics of the systems at both room and physiological temperatures. All data were obtained with the software provided by Malvern Instruments.

For a bicellar sample, the structure is discoidal, and a simple transformation from hydrodynamic radius (Rh) to particle radius (r, disk radius) is not evident. This transformation was carried out according to the equation given by Mazer et al. (13), which relates Rh with r:

$$Rh = 3/2r\Big(\left[1 + (t/2r)^2\right]^{1/2} + 2r/t\,\ln \times \left[t/2r + \left[1 + (t/2r)^2\right]^{1/2}\right] - t/2r\Big)^{-1}$$

For the disk thickness (t), we used a fixed value of 5.4 nm based on a previous work (4). To transform the intensity to volume, and considering the small disk radius and small refractive index differences, the Rayleigh-Debye-Gans approximation (14) and the form factor for disks proposed by Mazer et al. (13) were used.

Cryo-TEM

The preparations of liposomes and bicelles were visualized by the Cryo-TEM method. A thin, aqueous film was formed by dipping and withdrawing a bare specimen grid from the suspension. Glow-discharged, holey carbon grids were used. After withdrawal from suspension, the grid was blotted against filter paper, leaving thin sample films spanning the grid holes. These films were vitrified by plunging the grid into ethane, which was kept at its melting point by liquid nitrogen (15) using a Vitrobot (FEI, Eindhoven, The Netherlands), and by keeping the sample before freezing at 100% humidity. The thin films were vitrified at room temperature. The vitreous sample films were transferred to a Tecnai F20 microscope (FEI) using a cryotransfert (Gatan, Barcelona, Spain). The visualization was performed at 200 kV, at a temperature between −170°C and −175°C, under low-dose imaging conditions.

In vivo experiments: contrast agent visualization by MRI

Animals

MRI experiments were performed on adult male Wistar rats (Charles River, Lyon, France) weighing 250–275 g. The rats were housed under controlled temperature (21 ± 1°C) and humidity (55 ± 10%), with a 12-h light/12-h dark cycle (light between 6:00 AM and 6:00 PM). Food and water were available ad libitum. All experiments were performed in accordance with the National Institutes of Health animal protection guidelines and were approved by the local governmental authorities.

Stereotaxic injections

The animals were initially anesthetized with 4% isoflurane in O_2:N_2O (3:7), which was reduced to 1% isoflurane for maintenance. They were then placed in a stereotactic apparatus with a flat skull (Stoelting, Wood Dale, IL). The bregma, the sagittal suture, and the surface of the brain were used as references for the anterior-posterior (AP), medio-lateral (ML), and dorso-ventral (DV) coordinates, respectively. A hole was drilled in the skull for solution injection into the lateral ventricle at the following stereotaxic coordinates: AP: −0.04 mm; ML: −0.12 mm; DV: −0.37 mm from the bregma (16). Fifty microliters of an aqueous solution containing two different preparations of bicelles mixed with gadodiamide were injected via a 100-μL Hamilton syringe fitted with a 32-G needle at a rate of 2 μL/min. After injection, the needle was left in place for 5 min to prevent leakage. At the end of the surgery, the skin was sutured and the animal was moved to the scanner cradle for MRI. Three solutions containing gadodiamide (in bicelles, bicosomes, and a control sample of liposomes) were injected. The concentration of bicelles used for injection was 200 mg/mL. The researcher who conducted the stereotaxic administration was highly experienced in this procedure.

In vivo MRI

MRI scans were performed under isoflurane anesthesia in a BioSpec 70/30 horizontal animal scanner (Bruker BioSpin, Ettlingen, Germany) equipped with a 12-cm inner diameter, actively shielded gradient system (400 mT/m). The coil configuration consisted of a transmit/receive quadrature volume coil. The animals were placed in a supine position in a Plexiglas holder with a nose cone for administering anesthetic gases, and fixed by means of a tooth bar, earplugs, and adhesive tape. Tripilot scans were used to accurately position the animal's head inside the magnet. The animal's head was positioned such that the approximate center of the brain was located at the magnet's isocenter. T1-weighted axial and sagittal images were acquired using a conventional fast low-angle shot imaging sequence. The scan parameters for the sagittal images were as follows: repetition time (TR) = 350 ms, echo time (TE) = 5.4 ms, two averages, slice thickness = 1 mm, number of contiguous slices = 15, field of view (FOV) = 4×4 cm^2, and matrix = 256×256×15 pixels, resulting in a spatial resolution of 0.156×0.156 mm with a 1-mm slice thickness. In addition, T1 maps with axial orientation were acquired using a rapid acquisition with relaxation enhancement and variable time of repetition sequence. The scan parameters were TR = 182.412 ms, 200 ms, 500 ms, 700 ms, 1000 ms, 1400 ms, 2000 ms, 3000 ms, and 6000 ms; TE = 10 ms; slice thickness = 1 mm; number of contiguous slices = 12; FOV = 3×3 cm^2; and matrix = 128×128×12 pixels, resulting in a spatial resolution of 0.234×0.234 mm with a 1-mm slice thickness. This image acquisition was performed just after the injection and 4 h, 8 h, and 24 h later.

Image analysis

One ROI was drawn in the CSF compartment of each image to evaluate the signal enhancement produced by gadodiamide. Signal normalization was performed by dividing the mean signal intensity in the CSF ROI by the mean signal in the tongue muscle. Statistical analysis was performed using Student's paired t-test, and a value of $p < 0.05$ was considered significant.

RESULTS

Characterization of systems

Bicellar systems

The HD and the proportion of the particle populations were obtained by DLS and analyzed by intensity and by volume of light scattered. The data obtained at room temperature are shown in Table 1. The HDs for the DPPC/DHPC bicelles (Bice) were 19.5 nm and 16.3 nm, estimated by intensity and volume, respectively, with a proportion of the light scattered higher than 90% in both analyses.

TABLE 1 HD and proportion of the particle populations analyzed by intensity and by volume of light scattered

		Intensity		Volume	
		HD (nm)	% Intensity	HD (nm)	% Volume
Bice	Peak 1	19.5	91.3	16.3	93.9
Bico	Peak 1	489	100	571	100
Bice Dil	Peak 1	255	88.4	256	3.6
	Peak 2	26.8	11.6	26.6	96.4
Bico Dil	Peak 1	800	86.3	850	59.8
	Peak 2	72.4	13.7	68.7	40.2

The sample containing bicelles was diluted from 20% (initial concentration) to 0.07% (final concentration) to determine the effect of dilution on the bicellar structure. When this sample was diluted (Bice Dil), two populations (one ~26 nm and one ~255 nm) were observed for both analyses (by intensity and volume). The proportions of light scattered, analyzed by intensity and volume, were different. This is because large and small particles contribute differently to the intensity of scattered light. Large particles scatter light at a higher intensity than small particles (17). For this reason, in systems that are heterogeneous in size, an analysis by intensity inflates the proportion of large particles, as shown in Table 1. The simultaneous analysis by volume indicated a higher proportion of small particles (26.6 nm) than large ones, indicating the predominant presence of small particles in the system, although the intensity of light scattered by large particles was higher than that scattered by the small ones.

The values of PI for the bicellar systems were 0.452 and 0.714 before and after dilution, respectively. These results indicate that when the sample was diluted, the average size of the populations increased and the sample became more heterogeneous.

It is necessary to consider that with this technique, particle size is approximated to that of a hypothetical hard sphere that diffuses with the same speed as the particle under examination. Since the bicellar structure is disk-shaped, the particle size obtained by DLS provides a relative measurement of the structure dimensions. For this reason, the real disk diameter was calculated from the light-scattering results using the Mazer equation as described in Materials and Methods. The diameter obtained was 23.2 nm, similar to the HD result (19.5 nm; see Table 1). In addition, the size distribution by intensity was transformed to the size distribution by volume using the Rayleigh-Debye-Gans approximation and the form factor for disks, giving a diameter of 15.2 nm. This value is also on the order of the HD obtained by volume (16.3 nm; see Table 1). All of the measurements by DLS were obtained at 25°C and 37°C, and no modification in size was detected from a temperature effect. Given that temperature had no effect on these systems, cryo-TEM experiments were performed only for samples that had been cryofixed at room temperature. The images obtained offer a direct visualization of the bicellar systems.

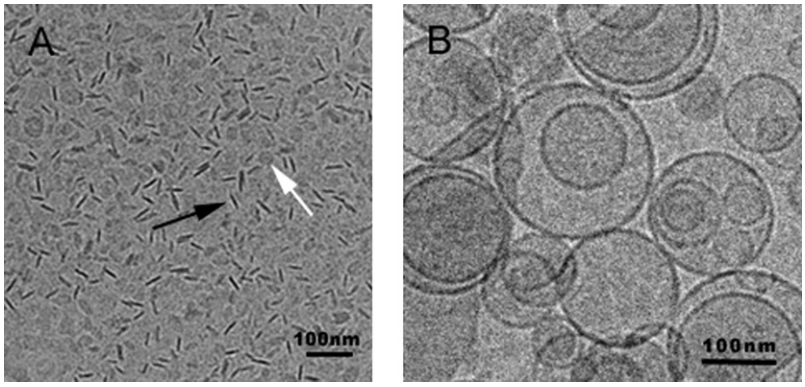

FIGURE 1 Representative micrographs of the samples before (*A*) and after (*B*) dilution. (*A*) Bice sample: discoidal structures (bicelles) are shown in all projections, face-on (*white arrow*) and edge-on (*black arrow*). (*B*) Bice Dil sample: spherical unilamellar vesicles.

Representative micrographs of the samples before (Bice) and after (Bice Dil) dilution are shown in Fig. 1, *A* and *B*, respectively. The images confirm the results obtained by DLS, showing that the structures in the Bice samples are smaller than those in the Bice Dil samples. In addition, the morphology of the particles changes with the dilution. In the Bice samples (Fig. 1 *A*), discoidal bicelles are shown in all projections, face-on (*white arrow*) and edge-on (*black arrow*), although the most evident is the edge-on projection. From the structures observed face-on, it may be assumed that the disks have a roughly circular shape. In addition, the disks exhibit diameters of ~20 nm, confirming the results obtained from DLS for the disks. In Fig. 1 *B* (Bice Dil samples), spherical unilamellar vesicles showing a great variety of sizes (from 30 to 250 nm) are observed. This agrees with the high PI (0.714) observed by DLS. Therefore, both the DLS and microscopy results indicate a transition of bicellar systems from disks to vesicles caused by the effects of dilution.

Liposomes encapsulating bicelles (bicosomes)

The DLS results for bicosomes (Bico) are shown in Table 1 (values obtained at room temperature). Only one peak, around 500 nm, was observed in the analyses by intensity and by volume, and both analyses yielded a proportion of light scattered of 100%.

When the sample was diluted (Bico Dil), two peaks were clearly observed (Table 1). The structures became larger, with diameters of 800 nm (86.3%) and 72.4 nm (13.7%) by intensity, and 850 nm (59.8%) and 68.7 nm (40.2%) by volume. The values of PI also increased from 0.259 to 0.612 before and after dilution, respectively. DLS data acquired at 37°C showed no changes in comparison with results obtained at room temperature.

To investigate the morphology of these systems, the Bico and Bico Dil samples were analyzed by cryo-TEM. In this case, the samples for microscopic observation were also cryofixed only at room temperature. The cryo-TEM micrographs are shown in Figs. 2 and 3. In Fig. 2 (Bico sample), two kinds of structures are observed: one shows a small size of ~20 nm, and the other is larger at ~100–500 nm. Fig. 2 *A* shows an overview of the Bico sample in which bicosomes and a small number of nonencapsulated bicelles are seen. Fig. 2 *B* displays encapsulated bicelles, in their two projections (*white arrows*), and nonencapsulated bicelles (*black arrows*). Some encapsulated bicelles exhibit an increase in size (~100 nm) with respect to the nonencapsulated bicelles (20 nm) (Fig. 2 *A*). In addition, face-to-face stacking bicelles were detected inside liposomes (Fig. 2 *C*). These micrographs report additional information that was not provided by the DLS results for Bico samples. Only

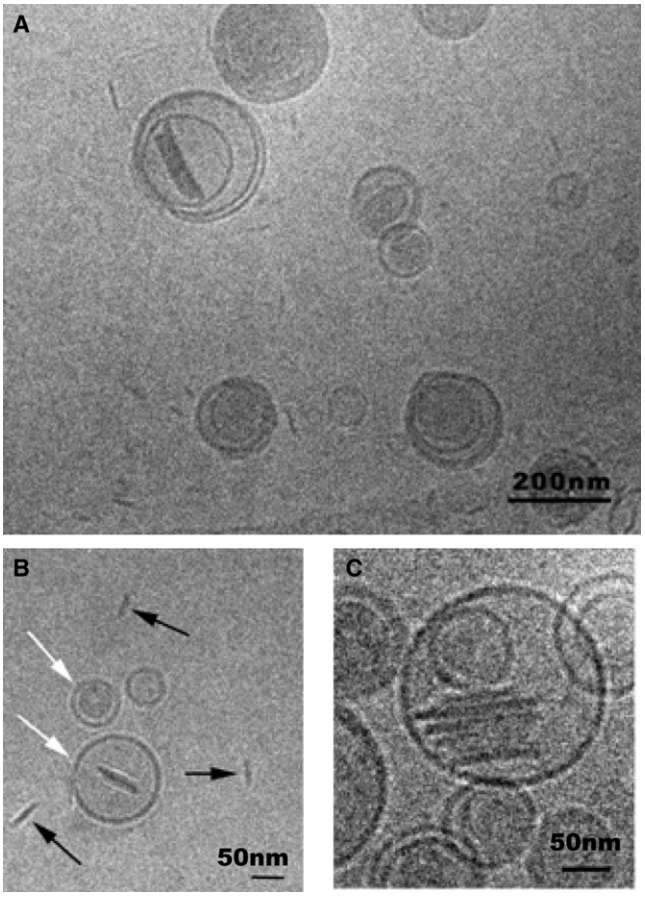

FIGURE 2 Cryo-TEM images of a Bico sample. (*A*) Bicosomes and bicelles are shown. (*B*) Encapsulated bicelles are observed, in their two projections (*white arrows*) and nonencapsulated bicelles (*black* arrows). (*C*) Stacks of bicelles adhered in parallel orientation are shown.

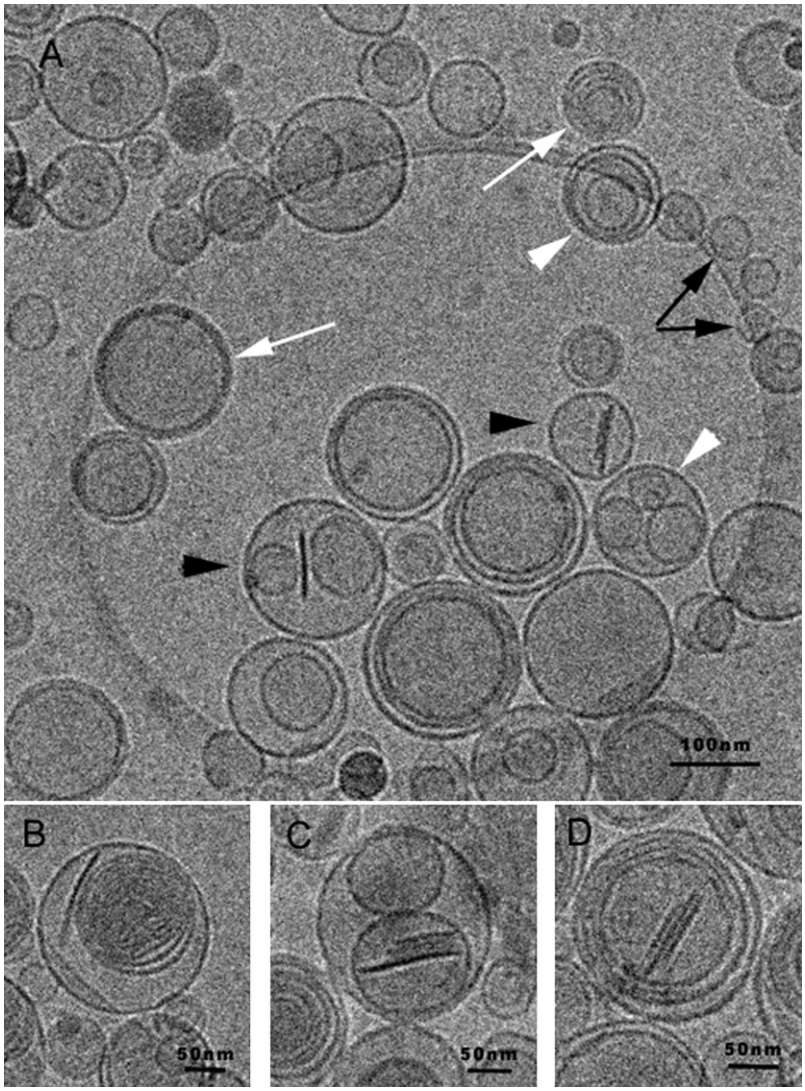

FIGURE 3 Cryo-TEM images of a Bico Dil sample. (*A*) High variability of vesicles is observed: empty liposomes (*black arrows*); liposomes inside other liposomes (oligolamellar (*white arrowheads*) and multilamellar vesicles (*white arrows*)); and liposomes with bicelles inside (*black arrowheads*). (*B*) Multilamellar liposomes. (*C*) Stacked bicelles inside liposomes. (*D*) Stacked bicelles inside multilamellar liposomes.

one peak was detected by the volume and intensity analyses (Table 1), but two types of structures were visualized by microscopy. In terms of DLS, it is probable that large particles (500 nm) scatter light at such an intensity that the light scattered from the small particles is imperceptible. The high contribution of large particles could hide the small contribution of the small particles. Therefore, two kinds of structures are probably present, even though only one peak was observed by DLS analysis.

When the sample was diluted (Bico Dil), only bicelles were observed inside liposomes; no free bicelles were visualized. Various vesicles were observed in this dilute sample (Fig. 3 *A*), including empty liposomes (*black arrows*), liposomes inside other liposomes (called oligolamellar vesicles; *white arrowheads*) and multilamellar vesicles (*white arrows*), and liposomes with bicelles inside (bicosomes; *black arrows*). Some details are shown in Fig. 3, *B–D*. Multilamellar liposomes are observed in Fig. 3, *B*, and Fig. 3 *C* shows stacked bicelles inside liposomes, as in the predilution samples (Fig. 2 *C*). This fact indicates that encapsulated bicelles did not undergo changes after dilution. A detail of stacked bicelles inside multilamellar liposomes is shown in Fig. 3 *D*. The great size variety of the structures in these images, from 70 nm to 600 nm, confirms the high PI (0.612) obtained by DLS in the Bico Dil samples. Our results indicate that the encapsulated bicelles are structurally preserved independently of the dilution process.

Control liposomes containing gadodiamide resulted in an HD of ~800 nm and a PI of 0.246.

In vivo experiments: MRI visualization

Intracerebroventricular injection of gadodiamide-bicelles

Intracerebroventricular (i.c.v.) injections were performed in two rats to observe the enhancement of signal intensity in the CSF induced by gadodiamide (contained in the different systems), as explained in detail in Materials and Methods. Five minutes after the end of the i.c.v. infusion of free

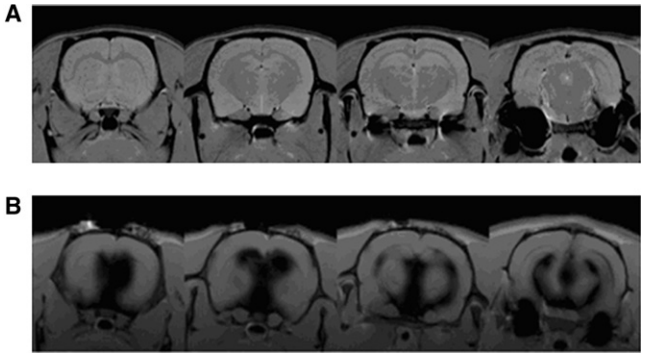

FIGURE 4 (*A*) Coronal view of a healthy rat brain. (*B*) Coronal view of a rat brain injected with bicelles containing gadodiamide. This rat died after the injection. The expansion of the ventricular system is noted.

bicelles, both animals died, and MRI was performed postmortem. Fig. 4 shows coronal views of the brains from control (*A*) and Bice-injected (*B*) rats. As can be observed in Fig. 4 *B*, free bicelles (Bice sample) caused a dramatic expansion of the whole cerebroventricular system of the rat.

Intracerebroventricular injection of gadodiamide-bicosomes

I.c.v. injections were also performed in rats to observe gadodiamide enhancement of signal intensity in the CSF by administration of Bico samples. The rat was injected as described above. Immediately after (0 h) and 4 h, 8 h, and 24 h later, the animal was scanned. In contrast to the case with the Bice sample, the animal that received the Bico sample survived, and this preparation had no apparent toxic effect. We found an increase in the signal intensity in the CSF after infusion of the Bico preparation. Fig. 5 *A* shows a sagittal view of the brain of a healthy rat (first image) and a Bico-injected rat 0 h, 4 h, 8 h, and 24 h after the injection (next four images). The gadodiamide-induced hyperintensity was quantified by drawing one ROI within an anatomic zone containing CSF at each time point (see Fig. 5 *B*) and plotted to observe its time course (Fig. 5 *C*). A time-dependent effect was observed, with the maximum hyperintensity in the scan performed directly after the infusion. A progressive decrease of the signal was observed. Twenty-four hours after infusion, the intensity was similar to that found in a control, noninjected animal.

A control experiment with an injection of gadodiamide entrapped in liposomes was performed, and the results were similar to those obtained from the injection of gadodiamide in the Bico samples.

DISCUSSION

Temperature effect on bicelles

Several factors affect the morphological stability of bicellar systems (18–20). Temperature and hydration are key parameters in determining the formation of a specific structure. A number of works have reported on the structural transitions of bicellar systems formed by DMPC/DHPC at temperature ranges similar to those used in this work (18,21). These transitions involved morphological changes in the structures from disks to cylindrical micelles, perforated lamellar sheets, and mixed multilamellar vesicles (22). However, the systems studied here did not exhibit such behavior, and in contrast showed (by DLS) the same size distribution at 25°C and 37°C. This is because the temperatures under study were below the DPPC T_m (41°C), and because in bicellar systems, phase transitions take place from the T_m (23–25). For this reason, systems containing DMPC (with T_m = 23°C) showed structural modifications between 25°C and 37°C. The long-chain phospholipid chosen in this study was DPPC precisely because the T_m value of this lipid is higher than physiological temperature. This ensured the structural and morphological stability of the systems against temperature effects. In any case, given the interest of these systems and considering the fluid state exhibited by DMPC at physiological temperature, which promotes increased stratum corneum permeability (5), other compositions of bicelles could be considered in future studies.

Dilution effect on bicelles

Another factor that, in general, induces morphological changes in bicelles is modification of the total lipid

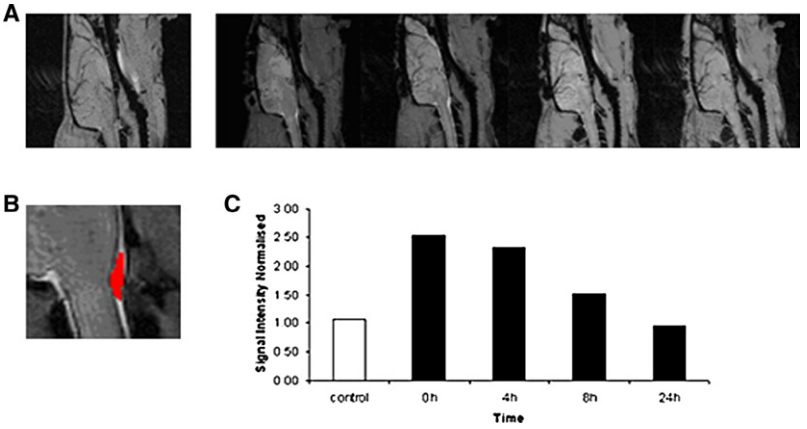

FIGURE 5 (*A*) Sagittal view of a healthy rat brain (first image) and a rat injected with bicelles containing gadodiamide inside liposomes (Bico sample), scanned at 0 h, 4 h, 8 h and 24 h after the injection. (*B*) Detail of the ROI used to monitor the time course of the hyperintensity induced by the contrast agent. (*C*) CSF signal intensity (normalized to muscle intensity) for a control rat (*white bar*) and for the rat injected with bicelles containing gadodiamide inside liposomes (*black bars*) at different time points after the injection.

concentration (20,26). In our work, this modification took place when the bicellar systems were diluted. Dilution promoted the growth of structures (Table 1) and the transition from discoidal bicelles to vesicles (Fig. 1). A recent study using freeze-fracture electron microscopy also indicated this tendency (4). However, that technique involves a Pt/C replication process for the samples, which can hinder visualization of structures smaller than 10 nm. Therefore, we considered cryo-TEM, which permits direct visualization of small structures, to be much more appropriate for evaluating our systems. It is noteworthy that the phase transitions of discoidal bicelles due to the variation of water content (or total lipid concentration) are very similar to those involved in reconstituting the surfactant-lipid micellar systems in vesicles (27–29). A model for the micelle-to-vesicle transition proposed by Leng et al. (30) describes the rapid formation of discoidal aggregates and their growth and closure to form vesicles. The resemblance between surfactant-lipid micelles and phospholipid bicelles justifies their similar behavior. Molecules of DHPC solubilize the DPPC bilayer, forming discoidal bicelles in a manner similar to the way in which surfactant molecules solubilize lipid vesicles and form micelles. In systems containing discoidal bicelles, DHPC molecules are partitioned between the discoidal structure (mainly in the edges) and the water (as monomers). When the water content increases (dilution), the concentration of DHPC in water decreases, and then DHPC is removed from the bicelles to let in the water. This phenomenon and the high hydrophobicity of the DPPC molecules induce an increase in the molar ratio (q) of structures, and as a consequence, the disk diameter increases. High-dilution conditions lead to the fusion and closure of large bilayered disks, and hence the formation of vesicles such as those shown in Fig. 1 *B*.

Relevance of bicosomes

It is reasonable to think that the isolation of bicelles from the medium would protect these nanostructures from the effect of posterior dilutions. This is precisely the strategy we propose here. Bicelles are encapsulated in lipid vesicles or liposomes, resulting in new nanostructures that we call bicosomes. Dilution of these systems does not affect the encapsulated bicelles (Fig. 3). The exterior lipid membrane ensures the isolation and stability of the bicelles captured in the interior; that is, the perfect microenvironment for the discoidal bicellar system is created inside the lipid vesicles. Liposomes have the advantage of being stable with temperature changes, and have a controllable size that is not altered by dilution. Previous studies have reported the usefulness of these lipid vesicles as biocompatible and protective structures to encapsulate labile molecules, such as proteins, nucleic acids, or drugs, for pharmaceutical, cosmetic, or chemical applications (30). Other methods have been used to stabilize the morphology of discoidal bilayers, such as using bicelles with charged amphiphiles (31) or disks formed by mixtures containing polyethylene glycol-lipid conjugates (PEG-lipids) (32). PEG-lipids have interesting applications, especially when drugs are included in discoidal bicelles. However, with the use of PEG-lipids, the properties of bicelles related to structural versatility, such as the enhancer effect of the permeability on some physiological barriers, could be lost. This enhancer effect of bicelles has been studied for skin purposes and is potentiated by discoidal structures formed with lipid mixtures in which the alkyl chains are sufficiently different in length (5,33). Bicelles formed with PEG-lipids are sterically stabilized, and all lipids that form these nanostructures have the same or very similar alkyl chain lengths (32).

The only difference between bicelles that are free in solution and those trapped in vesicles is an increase in the diameter of the latter and subsequent stacking. The difference in size, which is demonstrated in Figs. 1 *A* and 2, is maintained after the dilution of bicosomes (Fig. 3). This is probably related to a slight modification in the composition of the initial bicelles during the formation of the bicosomes. To form bicosomes, the lipid film, which is composed mainly of Lipoid phospholipids, is hydrated with the initial solution of preformed bicelles. At this step, and given the characteristics of these Lipoid lipids (long alkyl chain), a portion of the lipids of the film could be incorporated in the bilayer of the disks. In a similar way, a portion of the lipids of bicelles could be incorporated in the external membrane of bicosomes. In water, DHPC exhibits a critical micellar concentration of 15 mM (34), which is comparable to that of some mild surfactants, such as octyl glucoside ($\approx$18 mM (28)). Therefore, a certain solubilization of the external membrane could be suggested. However, the amount of DHPC incorporated in the external bilayer was not enough to solubilize the lipid membrane, as confirmed by cryo-TEM observations that were performed 10 days after preparation of the system. In any case, this lipid redistribution induces an increase in disk diameter. This increase in size is correlated with the strong tendency for these structures to stack inside the vesicles (35).

As mentioned above, the application of discoidal bicelles for skin purposes is being explored (3,5,33). The water content of the outermost layer of the skin is ~10–20%. Such low water content promotes the stability of discoidal bicelles and the interaction of these nanostructures with the skin. This interaction promotes effects related to an increased permeability of the barrier or a reinforcement of the skin lipids. Similar effects may also be expected in the interaction of discoidal bicelles with other tissues, although we are aware that the composition and physical properties of skin are different from those of other barriers (meaning that other interactions could occur). Moreover, the water content of the majority of tissues is usually too high to ensure the stability of the small disks. Our results confirm that the encapsulation of discoidal bicelles forming bicosomes preserves the

discoidal structures under dilution. Therefore, we believe that bicosomes are a good means of introducing bicelles in biological fluids with high water content, such as blood, CSF, and saliva. Bicosomes could be used as targeted vehicles to different barriers, such as endothelium (for intravenous administration) and gastric and intestinal mucosas (for oral administration). A possible interaction mechanism could be based on an initial interaction of the external Bico membrane with these barriers. At this point, the incorporation of PEG-lipids and the addition of antibodies to specific target sites in this external lipid bilayer seem necessary. Afterward, encapsulated bicelles could pass through different pathways (e.g., transcellular or paracellular) or by endocytosis by the M cells (36,37).

In our in vivo experiments, small discoidal bicelles and bicosomes (both with gadodiamide) were injected into rats. Injection of free bicelles killed the animals, whereas injection of bicosome samples did not. Due to the high water content of the CSF, both systems underwent a dilution process after injection, and contact with the CSF induced an increase in size. Although the size increase by the nanostructures after injection was not known, we assume that it was in the range indicated by our DLS results. Large-sized structures should not be lethal, as control liposomes exhibited sizes of ~800 nm and injection of these samples did not induce death. Moreover, larger structures have been used for similar in vivo studies (38). Another factor that allows us to discard the size as the cause of the animal's death was the fact that bicosomes become larger than bicelles after dilution, and only bicosomes permitted survival. Therefore, the toxicity of the bicelles may be due to the rapid morphological changes these structures undergo after they come into contact with the diluted environment of the CSF. This sudden and drastic morphological transition could form a lipid accumulation that obstructs the free flow of CSF and promotes the expansion of the cerebroventricular system. This expansion could cause compression of the brain stem, resulting in death, as previous works have observed with other methods (39,40). When the Bico sample was injected, the rat survived because large structures (bicosomes) that did not change with dilution were introduced together with a small amount of bicelles. Because only a small proportion of bicelles underwent a morphological transition, the lipid mass was not formed, and the obstruction of flow did not occur.

With regard to bicosomes as paramagnetic contrast agents, it is noteworthy that these nanostructures behave similarly to conventional lipid vesicles. Liposomes have been used as MRI contrast agents in two ways, according to the location of the paramagnetic complex (in the membrane or encapsulated in the liposome cavity (41)). Incorporation in the membrane is preferred because it achieves a more enhanced contrast for conventional liposomes applied intravenously (42). Other nanostructures based on micelles have also been used with the same purpose (43). In the work presented here, gadodiamide-DTPA (a water-soluble substance) was incorporated inside the vesicles together with the discoidal bicelles when the bicosomes were formed. This method showed an appropriate contrast, probably because the systems were injected intracranially. In addition, the incorporation of gadodiamide within vesicles is convenient because this process avoids the need to conjugate the gadodiamide to any hydrophobic molecule, so the paramagnetic probe can be used exactly as it is supplied for perfusion purposes.

CONCLUSIONS

This work describes a new strategy for stabilizing discoidal bicelles under diluted conditions. Bicosomes allow bicelles to reach other tissues, and the bicelles have an enhancer effect on skin permeability. These nanostructures could interact with other physiological barriers, and other interactions could occur. The incorporation of PEG-lipids and the addition of antibodies to specific target sites in the external lipid membranes is a logical next step. In addition, bicosomes could be used as stabilizers, since the bicelles trapped inside can be used to support various hydrophobic drugs, such as dichlofenac (6,7). In this sense, bicosomes work in a manner similar to that exhibited by other nanostructures, such as emulsions and multilamellar liposomes (44,45).

The combination of the well-known characteristics of liposomes with the versatility and applicability of bicelles makes bicosomes a unique multifunctional nanostructure.

The authors thank Txema Vicente, Sándalo Roldán-Vargas, and Ramon Pons for help with the particle size measurements. We also thank Orteve (Barcelona, Spain) for providing the lipids (Lipoid S-100).

This work was supported by funds from the Comisión Interministerial de Ciencia y Tecnología (CTQ 2007-60409) and Generalitat de Catalunya (GC BIOPOLIM-03086, 2005SR00066).

REFERENCES

1. Sanders, C. R., B. J. Hare, …, J. H. Prestegard. 1994. Magnetically oriented phospholipid micelles as a tool for the study of membrane associated molecules. *Prog. Nucl. Magn. Reson. Spectrosc.* 26:421–444.
2. Sanders, C. R., and J. H. Prestegard. 1990. Magnetically orientable phospholipid bilayers containing small amounts of a bile salt analogue, CHAPSOs. *Biophys. J.* 586:447–460.
3. Barbosa-Barros, L., C. Barba, …, O. López. 2008. Effect of bicellar systems on skin properties. *Int. J. Pharm.* 352:263–272.
4. Barbosa-Barros, L., A. de la Maza, …, O. López. 2008. Penetration and growth of DPPC/DHPC bicelles inside the stratum corneum of the skin. *Langmuir.* 24:5700–5706.
5. Rodríguez, G., L. Barbosa-Barros, …, O. López. 2009. Conformational changes in stratum corneum lipids by effect of bicellar systems. *Langmuir.* 25:10595–10603.
6. Guo, J., X. Tian, …, A. Makriyannis. 2008. Phospholipid Bicelle Membrane Systems for Studying Drug Molecules. Springer, Dordrecht, Netherlands.
7. Rubio, L., C. Alonso, …, O. López. 2010. Bicellar systems for in vitro percutaneous absorption of diclofenac. *Int. J. Pharm.* 386:108–113.

8. Teschke, O., and E. F. de Souza. 2002. Liposome structure imaging by atomic force microscopy: verification of improved liposome stability during adsorption of multiple aggregated vesicles. *Langmuir.* 18:6513–6520.

9. Zhao, J. M., Y. E. Har-el, …, P. C. van Zijl. 2008. Size-induced enhancement of chemical exchange saturation transfer (CEST) contrast in liposomes. *J. Am. Chem. Soc.* 130:5178–5184.

10. Hironaka, K., Y. Inokuchi, …, H. Takeuchi. 2009. Design and evaluation of a liposomal delivery system targeting the posterior segment of the eye. *J. Control. Release.* 136:247–253.

11. Chono, S., R. Fukuchi, …, K. Morimoto. 2009. Aerosolized liposomes with dipalmitoyl phosphatidylcholine enhance pulmonary insulin delivery. *J. Control. Release.* 137:104–109.

12. Kobayashi, H., S. Kawamoto, …, P. L. Choyke. 2006. Delivery of gadolinium-labeled nanoparticles to the sentinel lymph node: comparison of the sentinel node visualization and estimations of intra-nodal gadolinium concentration by the magnetic resonance imaging. *J. Control. Release.* 111:343–351.

13. Mazer, N. A., G. B. Benedek, and M. C. Carey. 1980. Quasielastic light-scattering studies of aqueous biliary lipid systems. Mixed micelle formation in bile salt-lecithin solutions. *Biochemistry.* 19:601–615.

14. Hofer, M. 1991. European Workshop on Neutron, X-Ray and Light Scattering as an Investigative Tool for Colloidal and Polymeric Systems P. Lindner and T. Zemb, editors. North Holland Delta Series, Amsterdam. 301–324.

15. Honeywell-Nguyen, P. L., P. M. Frederik, …, J. A. Bouwstra. 2002. Transdermal delivery of pergolide from surfactant-based elastic and rigid vesicles: characterization and in vitro transport studies. *Pharm. Res.* 19:991–997.

16. Paxinos, G., and C. Watson. 2007. The Rat Brain in Stereotaxic Coordinates. Elsevier, New York.

17. Barth, H. G. 1984. Modern Methods of Particle Size Analysis. Wiley-Interscience, New York.

18. Sternin, E., D. Nizza, and K. Gawrisch. 2001. Temperature dependence of DMPC/DHPC mixing in a bicellar solution and its structural implications. *Langmuir.* 17:2610–2616.

19. Dam, L. V., G. Karlsson, and K. Edwards. 2006. Morphology of magnetically aligning DMPC/DHPC aggregates-perforated sheets, not disks. *Langmuir.* 28:3280–3285.

20. Struppe, J., and R. R. Vold. 1998. Dilute bicellar solutions for structural NMR work. *J. Magn. Reson.* 135:541–546.

21. Hogberg, C. J., and A. P. Lyubartsev. 2006. A molecular dynamics investigation of the influence of hydration and temperature on structural and dynamical properties of a dimyristoylphosphatidylcholine bilayer. *J. Phys. Chem.* 110:14326–14336.

22. Harroun, T. A., M. Koslowsky, …, J. Katsaras. 2005. Comprehensive examination of mesophases formed by DMPC and DHPC mixtures. *Langmuir.* 21:5356–5361.

23. Lind, J., J. Nordin, and L. Mäler. 2008. Lipid dynamics in fast-tumbling bicelles with varying bilayer thickness: effect of model transmembrane peptides. *Biochim. Biophys. Acta.* 1778:2526–2534.

24. Sternin, E., T. Zaraiskaya, …, R. M. Epand. 2006. Changes in molecular order across the lamellar-to-inverted hexagonal phase transition depend on the position of the double-bond in mono-unsaturated phospholipid dispersions. *Chem. Phys. Lipids.* 140:98–108.

25. Loudet, C., S. Manet, …, E. J. Dufourc. 2007. Biphenyl bicelle disks align perpendicular to magnetic fields on large temperature scales: a study combining synthesis, solid-state NMR, TEM, and SAXS. *Biophys. J.* 92:3949–3959.

26. Yue, B., C. Y. Huang, …, J. Katsaras. 2005. Highly stable phospholipid unilamellar vesicles from spontaneous vesiculation: a DLS and SANS study. *J. Phys. Chem.* 109:609–616.

27. Goltsov, A. N., and L. I. Barsukov. 2000. Synergetics of the membrane self-assembly: a micelle-to-vesicle transition. *J. Biol. Phys.* 26:27–41.

28. López, O., M. Cócera, …, A. De la Maza. 2001. Octyl glucoside-mediated solubilization and reconstitution of liposomes: structural and kinetic aspects. *J. Phys. Chem.* 105:9879–9886.

29. Pinaki, R. M., and A. Blume. 2002. Temperature-induced micelle-vesicle transitions in DMPC-SDS and DMPC-DTAB mixtures studied by calorimetry and dynamic light scattering. *J. Phys. Chem.* 106:10753–10763.

30. Leng, J., S. U. Egelhaaf, and M. E. Cates. 2003. Kinetics of the micelle-to-vesicle transition: aqueous lecithin-bile salt mixtures. *Biophys. J.* 85:1624–1646.

31. Losonczi, J. A., and J. H. Prestegard. 1998. Improved dilute bicelle solutions for high-resolution NMR of biological macromolecules. *J. Biomol. NMR.* 12:447–451.

32. Johnsson, M., and K. Edwards. 2003. Liposomes, disks, and spherical micelles: aggregate structure in mixtures of gel phase phosphatidylcholines and poly(ethylene glycol)-phospholipids. *Biophys. J.* 85:3839–3847.

33. Rubio, L., C. Alonso, …, O. Lopez. 2010. Bicellar systems for in vitro percutaneous absorption of diclofenac. *Int. J. Pharm.* 386:108–113.

34. Martínez-Landeira, P., J. L. López-Fontán, …, F. Sarmiento. 2003. Surface behaviour of C5, C6, C7 and C8 lecithins at the aqueous solution/air interface. *Colloids Surf.* 216:91–96.

35. Bolze, J., T. Fujisawa, …, A. Naito. 2000. Small angle X-ray scattering and 31P NMR studies on the phase behavior of phospholipid bilayered mixed micelles. *Chem. Phys. Lett.* 329:215–220.

36. Fasano, A. 1998. Innovative strategies for the oral delivery of drugs and peptides. *Trends Biotechnol.* 16:152–157.

37. Spellerberg, B., S. Prasad, …, E. Tuomanen. 1995. Penetration of the blood-brain barrier: enhancement of drug delivery and imaging by bacterial glycopeptides. *J. Exp. Med.* 182:1037–1043.

38. Szoka, Jr., F. C., D. Milholland, and M. Barza. 1987. Effect of lipid composition and liposome size on toxicity and in vitro fungicidal activity of liposome-intercalated amphotericin B. *Antimicrob. Agents Chemother.* 31:421–429.

39. Kim, D. S., S. Oi, …, J. U. Choi. 1999. A new experimental model of obstructive hydrocephalus in the rat: the micro-balloon technique. *Childs Nerv. Syst.* 15:250–255.

40. Slobodian, I., D. Krassioukov-Enns, and M. R. Del Bigio. 2007. Protein and synthetic polymer injection for induction of obstructive hydrocephalus in rats. *Cerebrospinal Fluid Res.* 4:9.

41. Laurent, S., L. Vander Elst, …, R. N. Muller. 2008. Relaxivities of paramagnetic liposomes: on the importance of the chain type and the length of the amphiphilic complex. *Eur. Biophys. J.* 37:1007–1014.

42. Cheng, Z., and A. Tsourkas. 2008. Paramagnetic porous polymersomes. *Langmuir.* 24:8169–8173.

43. Shiraishi, K., K. Kawano, …, M. Yokoyama. 2009. Preparation and in vivo imaging of PEG-poly(L-lysine)-based polymeric micelle MRI contrast agents. *J. Control. Release.* 136:14–20.

44. Washington, C. 1996. Stability of lipid emulsions for drug delivery. *Adv. Drug Deliv. Rev.* 20:131–145.

45. Gaede, H. C., and K. Gawrisch. 2003. Lateral diffusion rates of lipid, water, and a hydrophobic drug in a multilamellar liposome. *Biophys. J.* 85:1734–1740.